SCIENCE CHINA Materials

ARTICLES

mater.scichina.com link.springer.com

Published online 10 July 2015 | doi: 10.1007/s40843-015-0069-7
Sci China Mater 2015, 58: 559–565

Organogel as durable anti-icing coatings

Yaling Wang[1,2], Xi Yao[1,2], Jing Chen[3], Zhiyuan He[1,2], Jie Liu[1,2], Qunyang Li[4], Jianjun Wang[1,2*] and Lei Jiang[1,2]

A durable organogel anti-icing material via swelling cross-linked poly(dimethylsiloxane) with liquid paraffin is reported. The surface of the organogel is covered by a thin released layer of paraffin due to the osmotic pressure, which acts as a lubricant and reduces the ice adhesion greatly. Results show that the ice adhesion on the surface of the organogel is as small as 1.7±1.2 kPa (at −30°C) and the low ice adhesion remains even when the temperature is lowered to −70°C. The surface with lubricating liquid paraffin layer exhibits excellent durability, as it shows an ultralow ice adhesion after 35 cycles of icing/deicing and 100 days of exposure in ambient environment.

INTRODUCTION

Ice formation and accretion on surfaces cause damages and inefficiencies that negatively impact aeronautics, ships, offshore oil platforms, power lines, wind turbines and telecommunication equipments [1]. Designing materials capable of efficiently minimizing or even eliminating the ice formation atop of their surfaces remains a challenge. Rendering the surfaces superhydrophobicity has been proposed as a leading passive anti-icing strategy because of the water repellency resulting from the high contact angle value and low ice adhesion strength due to the trapped air. However, superhydrophobicity would be lost at subzero temperatures because of the vapor condensation/desublimation [2–4]. Moreover, icing/deicing cycles may result in deterioration of superhydrophobicity (anti-icing properties) because of gradually breaking of the surface asperities [5–9]. Introducing a liquid lubricating layer between the ice and solid substrates is another strategy. Inspired by ice skating, Wang *et al.* prepared one type of self-lubricating liquid water layer created by hygroscopic polymer network deliquescing and swelling due to water absorption or condensation [10,11]. The temperature range, in which the self-lubricating liquid water layer exists, could be tuned by the water activity of the lubricating layer according to Koop *et al.* [12]. Another example is the development of lubricant-infused porous materials inspired by nature's *Nepenthes* pitcher plant which exhibits low contact angle hysteresis and has very low value ice adhesion (15.6 ± 3.6 kPa) [13,14]. However, for the passive removal of ice, the lower ice adhesion strength is, the better the anti-icing coating is [13]. This is particular true for the anti-icing of some outdoor facilities, and it would be ideal if the ice could be shed off due to its gravity or the action of wind. Organogel materials were found to have advantages for anti-sticking function by some researchers, since the polymer network merits a slow and continuous release of liquids [15–17]. Thus it should be useful for durable anti-icing coating. However no reports of organogel materials for anti-icing application have been reported.

Herein, we report an organogel (OG) anti-icing coating by swelling cross-linked polymer networks with liquid paraffin (LP). In this type of anti-icing coating, polymer network not only absorbs LP, but also holds the paraffin in the cross-linked network to avoid being abundantly removed during the shed off of the accreted ice [18,19]. We selected LP because it is a natural lubricant. LP-swollen cross-linked poly-dimethylsiloxane (PDMS) (LP-OG) is found to exhibit ultra-low ice adhesion strength (1.7 ± 1.2 kPa). Moreover the anti-icing coating can maintain effectively an ultra-low ice adhesion even when the temperature is as low as −70°C. Even after experiencing 35 icing/deicing cycles and 100 days of exposure in ambient environment, the ice adhesion on the LP-OG still keeps smaller than 10 kPa. All these indicate that LP-OG possesses a great potential for anti-icing coating with ultra-low ice adhesion, broad temperature window and excellent durability.

EXPERIMENTAL SECTION

Preparation of PDMS and organogel material

PDMS oligomer (Sylgard 184, Dow Corning) was mixed with the curing reagent at a ratio of 10:1 by weight to form a

[1] Institute of Chemistry, Chinese Academy of Sciences, Beijing 100190, China
[2] Graduate University of Chinese Academy of Sciences, Beijing 100049, China
[3] Department of Chemistry, School of Science, Tianjin University of Science and Technology, Tianjin 30045, China
[4] School of Aerospace, Tsinghua University, Beijing 100084, China
[*] Corresponding author (email: wangj220@iccas.ac.cn)

standard admixture. The resulting mixture was centrifuged at 5000 rpm for 5 min and then poured into a Petri dish with a thickness of 1.0 mm. Afterwards a vacuum (0.1 MPa) was applied for 30 min to remove all bubbles. The mixture was kept horizontally at room temperature for 24 h, and then cured in an oven at 80°C overnight. The cured PDMS was cut into square pieces (18 mm×18 mm), and immersed into heated paraffin bath for at least 7 h. Then the swelled PDMS pieces were taken out and cooled to room temperature and excess paraffin on the surface was removed. A liquid layer was formed on the surface of prepared organogel after it was kept overnight. Two kinds of paraffin were used in our experiments, i.e., LP and FT (Fischer-Tropsch wax). LP is commercial product which is liquid mixture of saturated cyclic hydrocarbon and isoalkane by refining process (molecular weight 250–450, melting point −24°C). FT is a kind of microcrystalline wax (melting point 102–104°C). Phenyl silicone (from silicone tube) and butyl rubber (from rubber plate) were swelled by LP following the procedure for the preparation of PDMS-based OG.

Ice adhesion measurement

The ice adhesion strength was tested by a home-built apparatus which consists of a cooling stage (experiment temperature ranges from −20 to −70°C) and an XY motion stage with force transducer as depicted in previous paper [3]. 1000 μL ultrapure water was syringed into a glass cuvette (10 mm × 10 mm × 25 mm) on organogel sample surface when the cooling stage reached a desired temperature. Ice columns formed and were kept at the same temperature for 5 h to ensure a full contact between the ice and the substrate. A nitrogen gas flow with a small flow rate purged continuously to avoid water vapor frosting on the substrate. Nine samples each time were measured. Probe velocity was 500 μm s^{-1} (typically used in other references) [20]. 50 μm s^{-1} was also tried to obtain some force curves in adhesion measurement. Non-shear contributions were minimized by keeping the probe distance constant (2 mm), as close to the surface as practical. Recorder for force-time curve was switch on just before the probe started to move. Once the probe contacted the glass cuvette that held the ice column, the force value began to increase until ice detachment. The probe continued to push the ice to slide and sliding friction force was also recorded. The shear force required for ice detachment was used to quantify ice adhesion force just before the adhesion failure. The contact area between the ice and the substrate was 1.00 cm^2. The ice adhesion strength (Pa) was obtained via dividing the shear force by the area. Ice adhesion strength has the same unit as the shear stress needed for ice detachment.

RESULTS AND DISCUSSION

Thermally-cured cross-linked PDMS was immersed in a bath of the heated LP. In order to reach swelling equilibrium, the PDMS network was soaked in the bath for 7 h. Then the PDMS was taken out and cooled down to room temperature. The prepared OG is transparent. Fig. 1a shows the images of PDMS before and after swollen by the LP. Kinetic process of swelling is described as the LP (as the solvent) diffusing into and out of the PDMS cross-linked structure driven by the osmotic potential (as interpreted by Flory-Huggins theory). LP is immiscible with the PDMS. But the affinity of the LP to PDMS makes a certain amount of LP impregnated in the cross-linked network of PDMS. Swelling is quick during the first 1.0 h and then the rate decreases gradually to reach a swelling limit (inset of Fig. 1a). Schott [21] used a second-order kinetic model to describe the diffusion-controlled swelling process and divided it into two stages: the diffusion of the solvent into a network and stress relaxation of the polymer network. The rate of former is faster than that of the later. The second-order kinetics can be expressed as

$$\frac{t}{Q_t}=\frac{1}{KQ_e^{\,2}}+\frac{t}{Q_e}. \tag{1}$$

Herein, Q_e is the equilibrium swelling ratio, Q_t is the swelling ratio of the moment t, K is the constant of rate. Fitted Q_e is 23.17 ± 2.41%. Lowering the temperature increases the viscosity of the solvent and decreases the relaxation degree of the network, resulting in a lower swelling ratio. This means that OG swelled by the LP will release LP at lower temperatures.

The optical microscopic image verifies the release of LP on the surface of LP-OG at room temperature as shown in Fig. 1b. Compared to the smooth and flat PDMS surface, the surface of LP-OG is covered by LP drops. Fig. 1c is the atomic force microscopy (AFM) images of PDMS and LP-OG surface. It shows that LP-OG has almost the same surface roughness as that of the PDMS surface. But AFM probe tip seems to skip always due to capillary interaction between the released LP on LP-OG surface and the AFM tip. Osmotic pressure and surface effect in combination result in the surface of OG being covered with a thin layer of LP. Released LP makes OG different from the PDMS surface. Static contact angle (CA) of water on LP-OG is slightly smaller than that on PDMS and the value decreases from 114.3 ± 0.5° to 108.6 ± 0.9°. This is reasonable since wax is reported to have lower Young's water contact angle than that of PDMS, which verifies that the released LP covers the surface of PDMS.

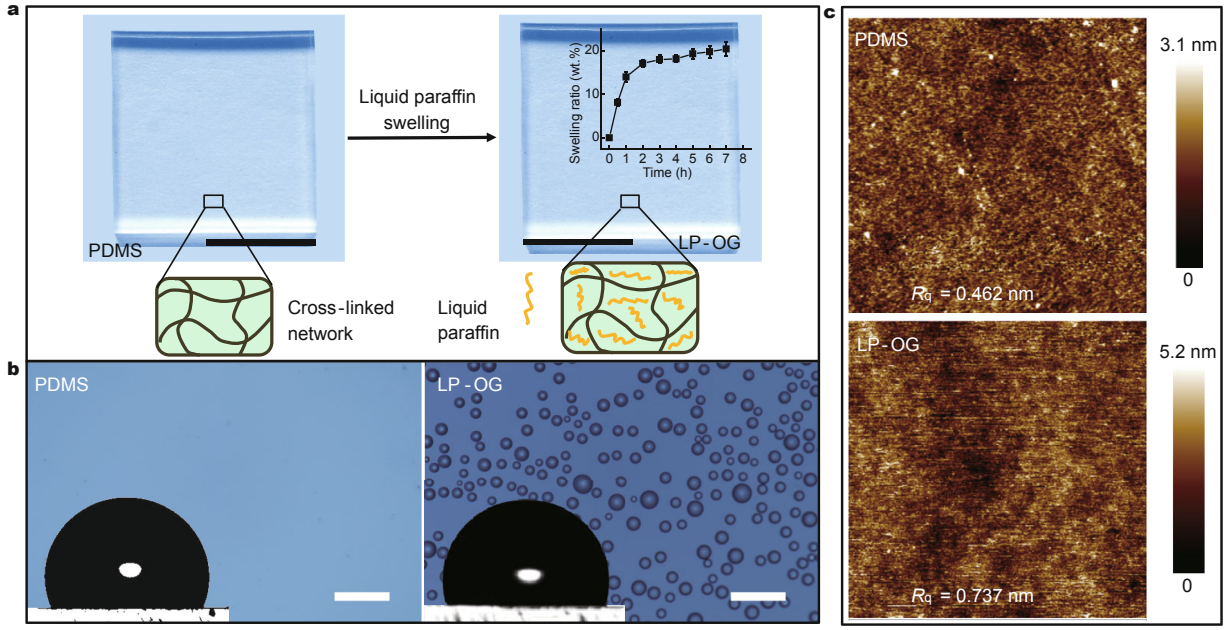

Figure 1 Preparation and surface release of LP-OG. (a) Images of cross-linked PDMS before and after being swollen by LP. The resulting OG was larger in size than the as-prepared PDMS due to swelling (scale bar is 1 cm). The swelling ratio of PDMS by LP changed with time and the equilibrium swelling ratio was obtained by fitting with Schott's second-order kinetics (inset). (b) Optical microscopic imaging of PDMS and LP-OG surface at room temperature. After releasing overnight, LP droplets come out onto the OG surface. Apparent CA of water drop on PDMS and LP-OG is 114.3 ± 0.5° and 108.6 ± 0.9°. Scale bar in the optical picture is 100 μm. (c) AFM images reveal that PDMS and LP-OG have almost the same surface roughness. Scan size is 10 μm × 10 μm.

Anti-icing performance of LP-OG is investigated by measuring the ice adhesion strength on the LP-OG surface. As shown in Fig. 2a, ice adhesion strength on the flat PDMS is 146.3 ± 9.3 kPa, which is in the range of values reported in the literature (about 120–460 kPa) [20]. PDMS with thickness of 533 μm has lower ice adhesion strength than that with thickness of 18 μm according to Kendall's theory $P_s \propto 1/t^{1/2}$ (t represents thickness of elastomer) [22]. PDMS swelled by LP has ultra-low ice adhesion strength of 1.7 ± 1.2 kPa, decreasing by almost two orders of magnitude compared to that of the PDMS. Other materials such as phenyl silicone and butyl rubber swelled by LP also reduce the ice adhesion strength by 60 and 20 times compared to that of dry polymer, with the ice adhesion of 2.0 ± 0.5 kPa and 7.8 ± 2.12 kPa, respectively. This verifies that LP-OG can decrease the ice adhesion greatly, thus can satisfy the passive removal of ice on the power line surface which usually requires ice adhesion strength smaller than 20 kPa [23,24].

To investigate the valid temperature range of the LP-OG for anti-icing, wide temperature range from −20 to −70°C was tested. Fig. 2b shows that ice adhesion strength on the PDMS surface is nearly independent on the temperature with a value around 150 kPa. On the LP-OG surface, ice adhesion strength maintains in the range of 1.7 ± 1.2–5.8 ± 1.8 kPa between −20 and −60°C and increases a little to 8.0 ± 3.7 kPa until −70°C. The increase of ice adhesion strength can be explained by the viscosity increase with the decrease of temperature. Previous research generally measured ice adhesion at −10°C or −15°C. Ice adhesion strength usually increases with the decrease of temperature [25]. Chen *et al.* [24] reported a sharp increase of ice adhesion strength from 55 ± 15 kPa to 1156 ± 152 kPa when temperature was cooled to −25°C, which signified the disappearance of the self-lubricating liquid water layer. The largest temperature range was reported by Dou *et al.* [11] who showed that polyurethane (PU-9) anti-icing coating maintained a low ice adhesion until the temperatures was lowered to −53°C, and then a sudden increase of the ice adhesion from 27 kPa to 200 kPa occurred. LP is a mixture of saturated alkane with reported melting point at −24°C. However, no sharp increase of ice adhesion was observed when the temperature was lowered below the melting point of LP. And the ice adhesion remained almost the same when the temperature was lowered to −70°C, which was the lowest temperature that our instrument can achieve. Therefore our LP-OG anti-icing coating has the largest temperature range reported in the literature.

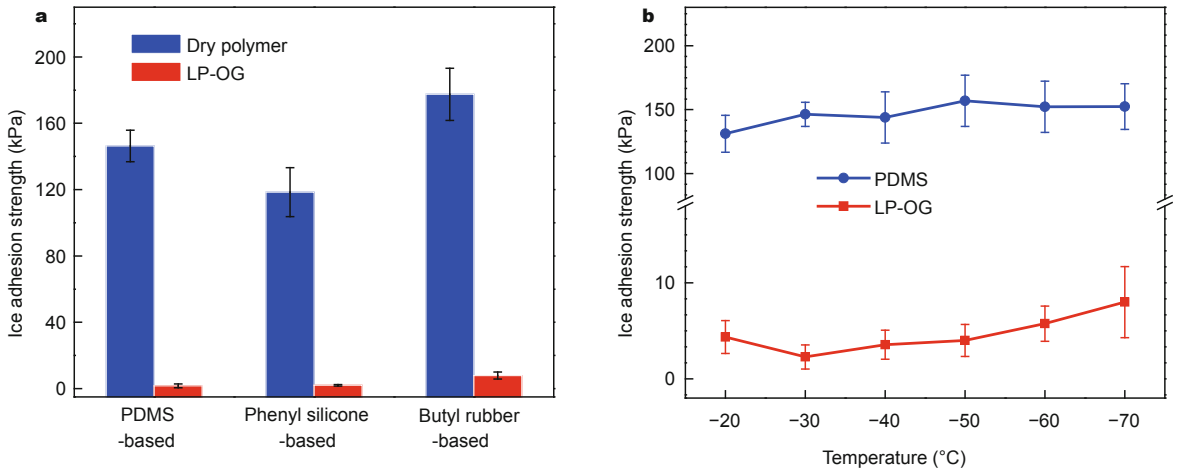

Figure 2 Anti-icing effect of LP-OG. (a) PDMS-based OG swelled by LP reduces the ice adhesion strength by 86 times compared to that of dry PDMS. Other polymer systems such as phenyl silicone and butyl rubber swelled by LP also show ultra-low ice adhesion strength. Measured at −30°C with a probe velocity of 500 μm s^{-1}. (b) Ice adhesion strength on LP-OG as temperature ranges from −20 to −70°C, which shows that LP-OG has the largest temperature range reported so far. In this paper, LP-OG is referred to PDMS-based if there is no special explanation.

Why do LP-OG surfaces show ultra-low ice adhesion strength with a large temperature window? Differential scanning calorimeter (DSC) curve shows that paraffin in LP bulk start to crystallize at about −20°C during the cooling process at a cooling rate of 5°C min^{-1}. After a complete crystallization at about −36°C, the total enthalpy change is 2.52 J g^{-1}. Enthalpy for the crystallization of pure paraffin is much higher (230.5–251.4 J g^{-1}) [26]. It means that only about 1.09% (by weight) paraffin crystallizes in LP. Under polarized optical microscope (inset), no visible crystals appear in the bulk LP, when the temperature is lowered from −20 to −70°C. As is known, LP contains saturated cycloalkane and isomerization alkane. Cyclic hydrocarbon with long side chain alkyl and isoalkane generally form small size and laminar crystals, while *n*-alkanes tend to form large size and fibrous crystals [27]. Phase transition temperature can be tuned by mixing light paraffin [28] and the size and morphology of the wax crystal can be varied by adding pour point depressant [29,30]. The component corresponding to phase transition at −24°C as shown in Fig. S1 should be some cyclic hydrocarbon or isoalkane. At low temperatures, only few crystals separated from LP, and the crystals are small and are separately embedded in the LP, thus LP bulk is actually still a liquid system. Low content of crystallizable components also cause the difficultness for the paraffin crystals being observed under polarized optical microscope.

When we mix LP with FT with ratios of 2:1 and 1:1 by weight, OG prepared by molten mixture swelling has ultra-low ice adhesion strength of 4.27 ± 0.92 kPa and 4.46 ± 0.82 kPa, even though solidified FT separates from LP on the released paraffin film on the OG surface. It indicates that a certain amount of solid paraffin does not disturb LP's anti-icing performance. It is possible to incorporate inorganic components to make composite anti-icing coatings, which is expected to increase the mechanical robustness. Low ice adhesion strength definitely requires the existence of lubricating layer, which property can be characterized by the equation,

$$F_k / A = \frac{\eta v}{h}, \quad (2)$$

where F_k is sliding friction on the thin fluid layer with contact area of A, η is the viscosity of fluid layer, v is the shear velocity, and h is the thickness of the fluid layer. For OG to have ultra-low ice adhesion (e.g., 2 kPa), only a thin LP layer with thickness of 2 μm is needed since LP has viscosity of 4000 mPa s (by rheometer-MCR 301, Anton Paar, Austria, with flow layer thickness of 1.000 mm at −30°C) and shear velocity of 500 μm s^{-1} [25,31].

Fig. 3b shows that force increases immediately to a maximum and ice is detached on the LP-OG surface. Then a non-zero force drives a dynamic sliding steadily. However, on the PDMS surface, force firstly experiences a slow increase and then reaches a maximum value to detach the ice. And then a drop of shear force down to zero follows. The difference between force dropping to non-zero and dropping to zero after the ice detachment verifies the liquid-like lubricating layer on LP-OG surface [32]. Dynamic sliding on PDMS surface shows a typical solid-like stick-slip friction characteristic. According to the Rabinowicz's model, it is typical for the sliding of a solid on an elastomer surface

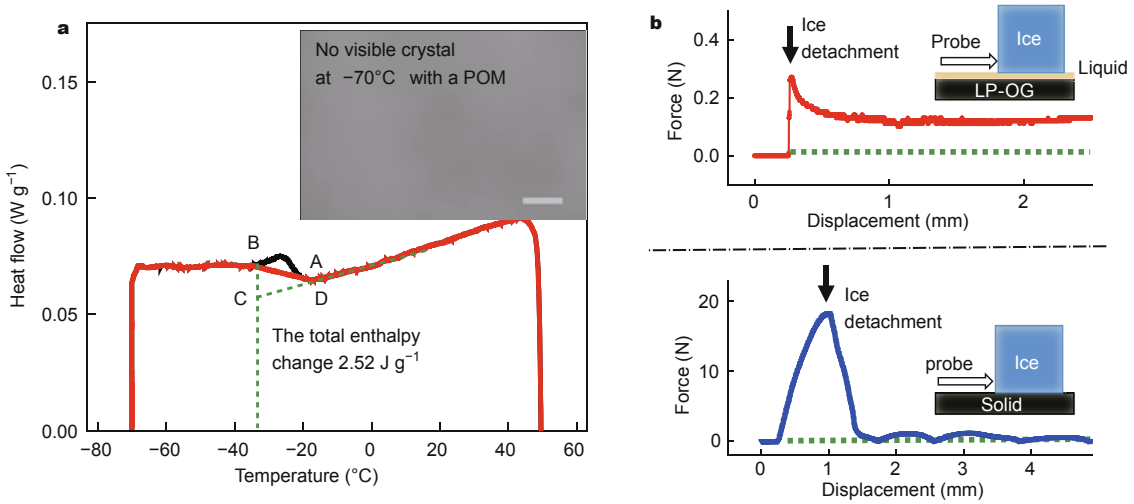

Figure 3 Ice adhesion mechanisms on the LP-OG surface. (a) DSC curve (black solid line) of LP during cooling process at a rate of 5°C min^{-1}. Red solid line is the virtual baseline. A and B are the start point and the end point of paraffin crystallization, respectively. The two gray dashed lines represent the end temperature of crystallization and extension of baseline before crystallization. Their intersection is the C point. D is the initial point of extension separating from red line and D is near A. The area of ABCD inclusion represents the enthalpy of paraffin crystallization. Inset is a polarized optical microscopic (POM) image of LP film sandwiched between two pieces of glass at −70°C. No visible crystal was observed during the cooling process from −20 to −70°C even to −150°C (scale bar 100 μm). (b) Force curves for ice adhesion measurement on the LP-OG surface (upper) and the PDMS surface (bottom) verify a liquid-like layer as a lubricant on the LP-OG. Ice adhesion force corresponds to the value in the curve at the moment of ice detachment marked by the black arrow. Gray dashed lines represent the zero-force baseline. The inset is the schematic illustration of the force measurement process.

[33]. On the LP-OG surface, static friction and smooth sliding represent a typical stop-start force-displacement curve for a simple liquid (driving velocity > critical velocity) [34]. While the friction force of liquid-like layers or films is lower and more like that of a viscous liquid flowing between two solid surfaces with a smooth friction [31,35]. As ice slides, the smooth sliding friction generally increases with sliding velocity as indicated in Equation (2), but the "effective" viscosity is usually much higher than the bulk viscosity of the trapped film [31]. When the film thickness becomes larger than 1 μm, viscosity of LP film is the same as that of the bulk [25]. Besides, before ice detachment, force on the LP-OG surface increases rapidly, which means that lubricating domains on OG and effect of elastic deformation can be neglected. The absence of stick-slip dynamics in the sliding friction indicates that no capillary bridges are formed for thin LP lubricating layer, which can exert its bulk fluidity [36]. Temperature dependence of ice adhesion on LP-OG comes from dependence of viscosity on temperature. Viscosity increase with temperature decrease from −20°C to −70°C explains the little increase in ice adhesion strength in Fig. 2b. In fact, ice adhesion force in shear is equal to the static friction. Fig. S2 provides an empirical value of $(F_s - F_k)/F_k = 0.5–2$ (F_s is the static friction, equal to ice adhesion force in the measurement), which relates ice adhesion force to viscosity and thickness of lubricating layer on LP-OG. Above result that thin LP layer with thickness of 2 μm is needed for 2 kPa is obtained based on this relationship.

The durability of anti-icing performance of LP-OG anti-icing materials was studied via the variation of ice adhesion strength with the icing/deicing cycle as well as the service time as shown in Fig. 4. LP-OG was tested by repeated icing/deicing for 100 days at ambient environment. During this period, it was exposed to the sunlight. The ice adhesion strength on the LP-OG surface showed very little increase after 35 cycles of icing/deicing. It is noteworthy that LP-OG's anti-icing performance is maintained after serving for one hundred days. When LP-OG reaches to swelling equilibrium after 7 h, the weight of captured LP is about 23.17 ± 2.41% of that of PDMS network. Due to the affinity of LP to PDMS, the release rate of LP-OG is slow compared to swelling. In addition, micrometer thickness is enough for lubricating according to Equation (2). Thus LP-OG has a long lifetime showing a promising candidate for anti-icing coating.

CONCLUSIONS

We prepared a durable OG anti-icing coating which is formed by swelling cross-linked polymer network with LP, and the released paraffin lubricating layer reduced the ice adhesion simultaneously. LP swelled PDMS network shows ultra-low ice adhesion strength. Moreover, the ice adhesion of the anti-icing coating remains ultra-low at the temperature as low as −70°C. Durability has been confirmed as the

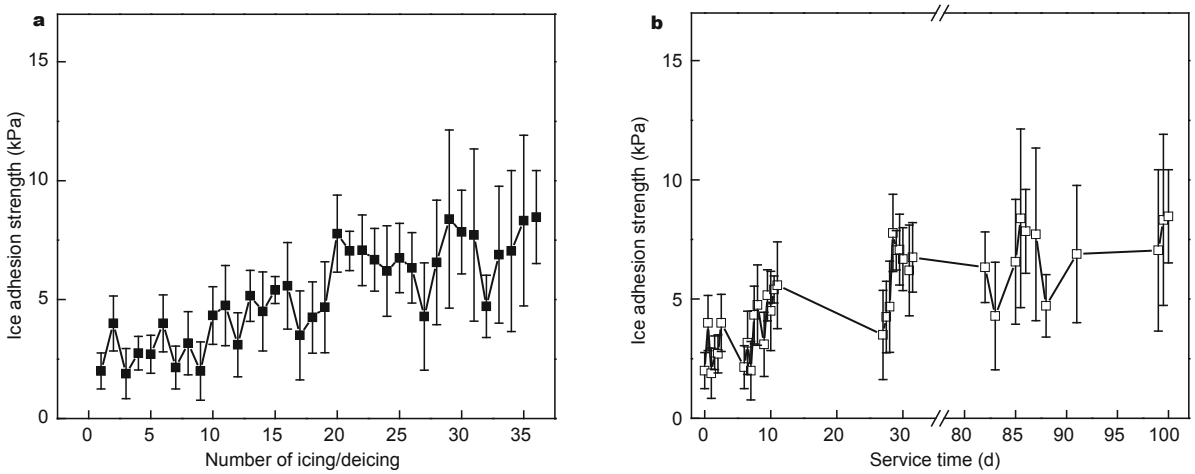

Figure 4 Durability of LP-OG for anti-icing. (a) Average ice adhesion strength on the surface of LP-OG at −30°C remains almost the same after several tens icing/deicing cycles. (b) Average ice adhesion strength *vs*. service time. It clearly shows that the fabricated anti-icing surfaces have favorable durability for anti-icing.

LP-OG coating is still valid after more than 35 times icing/deicing cycles during one hundred days of exposure in ambient environment.

Received 3 June 2015, accepted 24 June 2015
published online 10 July 2015

1 Meuler AJ, McKinley GH, Cohen RE. Exploiting topographical texture to impart icephobicity. ACS Nano, 2010, 4: 7048–7052
2 Varanasi KK, Deng T, Smith JD, *et al*. Frost formation and ice adhesion on superhydrophobic surfaces. Appl Phys Lett, 2010, 97: 234102
3 Chen J, Liu J, He M, *et al*. Superhydrophobic surfaces cannot reduce ice adhesion. Appl Phys Lett, 2012, 101: 111603
4 Kulinich SA, Farhadi S, Nose K, *et al*. Superhydrophobic surfaces: are they really ice-repellent? Langmuir, 2011, 27: 25–29
5 Farhadi S, Farzaneh M, Kulinich SA. Anti-icing performance of superhydrophobic surfaces. Appl Surf Sci, 2011, 257: 6264–6269
6 Lv J, Song YL, Jiang L, *et al*. Bio-inspired strategies for anti-icing. ACS Nano, 2014, 8: 3152–3169
7 Boinovich LB, Emelyanenko AM, Ivanov VK, *et al*. Durable icephobic coating for stainless steel. ACS Appl Mater Interfaces, 2013, 5: 2549–2554
8 Lazauskas A, Guobiene A, Prosycevas I, *et al*. Water droplet behavior on superhydrophobic SiO_2 nanocomposite films during icing/deicing cycles. Mater Character, 2013. 82: 9–16
9 Kulinich SA, Farzaneh M. On ice-releasing properties of rough hydrophobic coatings. Cold Reg Sci Technol, 2011, 65: 60–64
10 Chen J, Luo ZQ, Fan QR, *et al*. Anti-ice coating inspired by ice skating. Small, 2014, 10: 4693–4699
11 Dou R, Chen J, Zhang YF, *et al*. Anti-icing coating with an aqueous lubricating layer. ACS Appl Mater Interfaces, 2014, 6: 6998–7003
12 Koop T, Luo B, Tsias A, *et al*. Water activity as the determinant for homogeneous ice nucleation in aqueous solutions. Nature, 2000, 406: 611–614
13 Wong TS, Kang SH, Tang SK, *et al*. Bioinspired self-repairing slippery surfaces with pressure-stable omniphobicity. Nature, 2011, 477: 443–447
14 Kim P, Wong TS, Alvarenga J, *et al*. Liquid-infused nanostructured surfaces with extreme anti-ice and anti-frost performance. ACS Nano, 2012, 6: 6569–6577
15 Yao X, Hu Y, Grinthal A, *et al*. Adaptive fluid-infused porous films with tunable transparency and wettability. Nat Mater, 2013, 12: 529–534
16 Liu H, Zhang PC, Liu MJ, *et al*. Organogel-based thin films for self-cleaning on various surfaces. Adv Mater, 2013, 25: 4477–4481
17 Yao X, Ju J, Yang S, *et al*. Temperature-driven switching of water adhesion on organogel surface. Adv Mater, 2014, 26: 1895–1900
18 Subramanyam SB, Rykaczewski K, Varanasi KK. Ice adhesion on lubricant-impregnated textured surfaces. Langmuir, 2013, 29: 13414–13418
19 Rykaczewski K, Anand S, Subramanyam SB, *et al*. Mechanism of frost formation on lubricant-impregnated surfaces. Langmuir, 2013, 29: 5230–5238
20 Meuler AJ, Smith JD, Varanasi KK, *et al*. Relationships between water wettability and ice adhesion. ACS Appl Mater Interfaces, 2010, 2: 3100–3110
21 Schott H. Kinetics of swelling of polymers and their gels. J Pharm Sci, 1992, 81: 467–470
22 Wang C, Fuller T, Zhang W, *et al*. Thickness dependence of ice removal stress for a polydimethylsiloxane nanocomposite: Sylgard 184. Langmuir, 2014, 30: 12819–12826
23 Hejazi V, Sobolev K, Nosonovsky M. From superhydrophobicity to icephobicity: forces and interaction analysis. Sci Rep, 2013, 3: 2194
24 Chen J, Dou R, Cui D, *et al*. Robust prototypical anti-icing coatings with a self-lubricating liquid water layer between ice and substrate. ACS Appl Mater Interfaces, 2013, 5: 4026–4030
25 Jellinek HHG. Ice adhesion. Can J of Phys, 1962, 40: 1294–1309
26 Farid MM, Khudhair AM, Razack S, *et al*. A review on phase change energy storage: materials and applications. Energy Convers Manage, 2004, 45: 1597–1615
27 Pechook S, Pokroy B. Bioinspired hierarchical superhydrophobic structures formed by n-paraffin waxes of varying chain lengths. Soft Matter, 2013, 9: 5710–5715
28 Oró E, de Gracia A, Castell A, *et al*. Review on phase change materials (PCMs) for cold thermal energy storage applications. Appl Energy, 2012,99: 513–533
29 Liu LL, Wang B, Zhang SG. The depression mechanism and influ-

encing factors of pour point depressants for crude oil. Speciality Petrochem, 2006, 3: 020, in Chinese
30 Zhang JJ, Guan JN, Song N, *et al*. Influence of pour point depressant on wax crystal morphology of crude oil. Acta Petrolei Sinica (Petroleum Processing Section), 2010, 1: 006
31 Yoshizawa H, Chen YL, Israelachvili J. Fundamental mechanisms of interfacial friction. 1. Relation between adhesion and friction. J Phys Chem, 1993, 97: 4128–4140
32 Ge L, Ding GF, Wang H, *et al*. Anti-icing property of superhydrophobic octadecyltrichlorosilane film and its ice adhesion strength. J Nanomater, 2013, 2013: 278936
33 Yoshizawa H, Israelachvili J. Fundamental mechanisms of interfacial friction. 2. Stick-slip friction of spherical and chain molecules. J Phys Chem, 1993, 97: 11300–11313
34 Drummond C, Israelachvili J. Dynamic phase transitions in confined lubricant fluids under shear. Phys Rev E, 2001, 63: 041506
35 Gee ML, McGuiggan PM, Israelachvili JN, *et al*. Liquid to solid-like transitions of molecularly thin films under shear. J Chem Phys, 1990, 93: 1895–1906
36 Chen W, Foster AS, Alava MJ, *et al*. Stick-slip control in nanoscale boundary lubrication by surface wettability. Phys Rev Lett, 2015, 114: 095502

Acknowledgements The authors are grateful for the support from the National Natural Science Foundation of China (51173196, 51436004 and 21421061) and the National Basic Research Program of China (2012CB933801 and 2013CB933004).

Author contributions Wang J and Jiang L designed the experiments; Wang Y, Chen J, He Z and Yao X performed the experiments; Wang J and Li Q supervised the theoretical and experimental work. Wang Y, Chen J and Wang J wrote the manuscript. All authors contributed to the general discussion and reviewed the manuscript.

Conflict of interest The authors declare that they have no conflict of interest.

Supplementary information Supplementary data are available in the online version of the paper.

Yaling Wang is currently a PhD candidate at the Institute of Chemistry, Chinese Academic of Sciences. She obtained her MSc degree in environmental sciences from the University of Chinese Academy of Sciences in 2012. Her current research is anti-icing coating with ultra-low ice adhesion.

Jianjun Wang obtained his PhD degree at Max-Planck Institute for Polymer Research and the University of Mainz (Germany) in 2006. After seven months of postdoctoral research, he became a project leader at Max-Planck Institute for Polymer Research. Since 2010, he has been a professor at the Institute of Chemistry, Chinese Academic of Sciences. His current research interest is anti-icing materials.

中文摘要 本论文报道了一种通过液体石蜡溶胀聚二甲基硅氧烷制备持久耐用的油凝胶除冰涂层的方法. 由于油凝胶表面被一层渗透压驱动的石蜡缓释层覆盖, 这层缓释层可作为润滑层, 大大降低油凝胶表面的冰粘附强度. 实验结果显示, 油凝胶表面是一种具有超低冰粘附的防结冰材料, 在−30°C测试温度条件下的冰粘附强度是1.7 ± 1.2 kPa, 且温度降低到−70°C时, 其冰粘附强度不高于10 kPa. 在连续100天的使用期间, 经过35次的结冰/除冰循环操作, 具有润滑层的油凝胶表面仍然保持了持久的低粘附特性. 较低的冰粘附和较宽的低温适用窗口, 以及持久的耐用性, 使其在依靠重力或风力的低粘附被动除冰领域具有很大的潜力和实际应用价值.